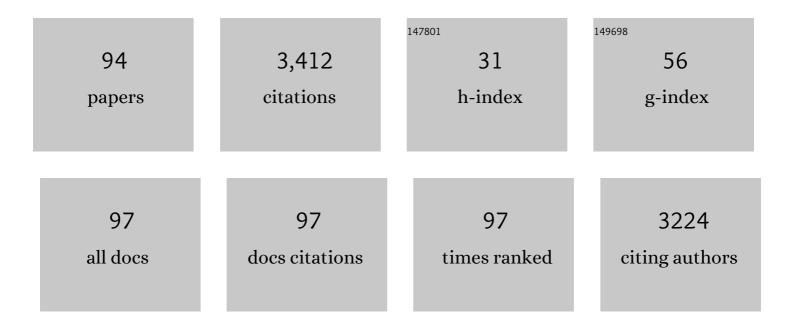
Jindrich Fanfrlik

List of Publications by Year in descending order

Source: https://exaly.com/author-pdf/2997073/publications.pdf Version: 2024-02-01



#	Article	IF	CITATIONS
1	Druggable Hot Spots in the Schistosomiasis Cathepsin B1 Target Identified by Functional and Binding Mode Analysis of Potent Vinyl Sulfone Inhibitors. ACS Infectious Diseases, 2021, 7, 1077-1088.	3.8	9
2	Azanitrile Inhibitors of the SmCB1 Protease Target Are Lethal to <i>Schistosoma mansoni</i> : Structural and Mechanistic Insights into Chemotype Reactivity. ACS Infectious Diseases, 2021, 7, 189-201.	3.8	9
3	Transformation of various multicenter bondings within bicapped-square antiprismatic motifs: <i>Z</i> -rearrangement. Dalton Transactions, 2021, 50, 12098-12106.	3.3	4
4	Structural and Thermodynamic Analysis of the Resistance Development to Pimodivir (VX-787), the Clinical Inhibitor of Cap Binding to PB2 Subunit of Influenza A Polymerase. Molecules, 2021, 26, 1007.	3.8	8
5	The Structure-Based Design of SARS-CoV-2 nsp14 Methyltransferase Ligands Yields Nanomolar Inhibitors. ACS Infectious Diseases, 2021, 7, 2214-2220.	3.8	57
6	Thiaborane Icosahedral Barrier Increased by the Functionalization of all Terminal Hydrogens in closo-1-SB11H11. Inorganic Chemistry, 2021, 60, 8428-8431.	4.0	1
7	SQM/COSMO Scoring Function: Reliable Quantumâ€Mechanical Tool for Sampling and Ranking in Structureâ€Based Drug Design. ChemPlusChem, 2020, 85, 2361-2361.	2.8	4
8	Unraveling the anti-influenza effect of flavonoids: Experimental validation of luteolin and its congeners as potent influenza endonuclease inhibitors. European Journal of Medicinal Chemistry, 2020, 208, 112754.	5.5	21
9	Electrophilic Methylation of Decaborane(14): Selective Synthesis of Tetramethylated and Heptamethylated Decaboranes and Their Conjugated Bases. Inorganic Chemistry, 2020, 59, 10540-10547.	4.0	3
10	Biomimetic Macrocyclic Inhibitors of Human Cathepsin D: Structure–Activity Relationship and Binding Mode Analysis. Journal of Medicinal Chemistry, 2020, 63, 1576-1596.	6.4	19
11	Bromination Mechanism of <i>closo</i> â€1,2â€C ₂ B ₁₀ H ₁₂ and the Structure of the Resulting 9â€Brâ€ <i>closo</i> â€1,2â€C ₂ B ₁₀ H ₁₁ Determined by Gas Electron Diffraction. ChemPlusChem, 2020, 85, 2606-2610.	2.8	6
12	Benchmark Data Sets of Boron Cluster Dihydrogen Bonding for the Validation of Approximate Computational Methods. ChemPhysChem, 2020, 21, 2599-2604.	2.1	4
13	SQM/COSMO Scoring Function: Reliable Quantumâ€Mechanical Tool for Sampling and Ranking in Structureâ€Based Drug Design. ChemPlusChem, 2020, 85, 2362-2371.	2.8	12
14	Faceâ€Fusion of Icosahedral Boron Hydride Increases Affinity to γâ€Cyclodextrin: closo , closo â€[B 21 H 18] â°' as an Anion with Very Low Free Energy of Dehydration. ChemPhysChem, 2020, 21, 971-976.	2.1	14
15	Optimization of norbornylâ€based carbocyclic nucleoside analogs as cyclinâ€dependent kinase 2 inhibitors. Journal of Molecular Recognition, 2020, 33, e2842.	2.1	2
16	The Influence of Halogenated Hypercarbon on Crystal Packing in the Series of 1-Ph-2-X-1,2-dicarba-closo-dodecaboranes (X = F, Cl, Br, I). Molecules, 2020, 25, 1200.	3.8	3
17	Complexation and stability of the fungicide penconazole in the presence of zinc and copper ions. Rapid Communications in Mass Spectrometry, 2020, 34, e8714.	1.5	8
18	Chalcogen Bonding due to the Exo-Substitution of Icosahedral Dicarbaborane. Molecules, 2019, 24, 2657.	3.8	6

#	Article	IF	CITATIONS
19	Thiaboranes on Both Sides of the Icosahedral Barrier: Retaining and Breaking the Barrier with Carbon Functionalities. ChemPlusChem, 2019, 84, 822-827.	2.8	4
20	A theoretical analysis of the structure and properties of B ₂₆ H ₃₀ isomers. Consequences to the laser and semiconductor doping capabilities of large borane clusters. Physical Chemistry Chemical Physics, 2019, 21, 12916-12923.	2.8	5
21	Thiaborane clusters with an exoskeletal B–H group. Chemical Communications, 2019, 55, 3375-3378.	4.1	1
22	Synthesis of <i>closo-</i> 1,2-H ₂ C ₂ B ₈ Me ₈ and 1,2-H ₂ C ₂ B ₈ Me ₇ X (X = I and OTf) Dicarbaboranes and Their Rearrangement Reactions. Inorganic Chemistry, 2019, 58, 2865-2871.	4.0	7
23	Investigation of Thiaborane <i>closo</i> – <i>nido</i> Conversion Pathways Promoted by <i>N</i> -Heterocyclic Carbenes. Inorganic Chemistry, 2019, 58, 2471-2482.	4.0	6
24	Nature of Binding in Planar Halogen–Benzene Assemblies and Their Possible Visualization in Scanning Probe Microscopy. Journal of Physical Chemistry C, 2019, 123, 8379-8386.	3.1	6
25	Icosahedral Carbaboranes with Peripheral Hydrogen–Chalcogenide Groups: Structures from Gas Electron Diffraction and Chemical Shielding in Solution. Chemistry - A European Journal, 2019, 25, 2313-2321.	3.3	16
26	A systematic examination of classical and multi-center bonding in heteroborane clusters. Physical Chemistry Chemical Physics, 2018, 20, 4666-4675.	2.8	26
27	Ranking Power of the SQM/COSMO Scoring Function on Carbonic Anhydraseâ€Il–Inhibitor Complexes. ChemPhysChem, 2018, 19, 873-879.	2.1	29
28	Various types of non-covalent interactions contributing towards crystal packing of halogenated diphospha-dicarbaborane with an open pentagonal belt. New Journal of Chemistry, 2018, 42, 10481-10483.	2.8	1
29	Sâ∢N chalcogen bonded complexes of carbon disulfide with diazines. Theoretical study. Chemical Physics, 2018, 500, 37-44.	1.9	12
30	Dihalogen and Pnictogen Bonding in Crystalline Icosahedral Phosphaboranes. Crystals, 2018, 8, 390.	2.2	16
31	Quantitative syntheses of permethylated <i>closo</i> -1,10-R ₂ C ₂ B ₈ Me ₈ (R = H, Me) carboranes. Egg-shaped hydrocarbons on the Frontier between inorganic and organic chemistry. RSC Advances, 2018. 8, 38238-38244.	3.6	6
32	Outerly functionalized and non-functionalized boron clusters intercalated into layered hydroxides with different modes of binding: materials for superacid storage. Dalton Transactions, 2018, 47, 11669-11679.	3.3	4
33	Methyl camouflage in the ten-vertex <i>closo</i> -dicarbaborane(10) series. Isolation of <i>closo</i> -1,6-R ₂ C ₂ 8 ₈ Me ₈ (R = H and Me) and their monosubstituted analogues. Dalton Transactions, 2018, 47, 11070-11076.	3.3	6
34	Chalcogen Bonding in Proteinâ^'Ligand Complexes: PDB Survey and Quantum Mechanical Calculations. ChemPhysChem, 2018, 19, 2540-2548.	2.1	50
35	SQM/COSMO Scoring Function at the DFTB3-D3H4 Level: Unique Identification of Native Protein–Ligand Poses. Journal of Chemical Information and Modeling, 2017, 57, 127-132.	5.4	40
36	Structural Basis of the Interaction of Cyclinâ€Dependent Kinaseâ€2 with Roscovitine and Its Analogues Having Bioisosteric Central Heterocycles. ChemPhysChem, 2017, 18, 785-795.	2.1	14

Jindrich Fanfrlik

#	Article	IF	CITATIONS
37	Binary twinned-icosahedral [B ₂₁ H ₁₈] ^{â^'} interacts with cyclodextrins as a precedent for its complexation with other organic motifs. Physical Chemistry Chemical Physics, 2017, 19, 11748-11752.	2.8	26
38	B–Hâ⊄Ï€: a nonclassical hydrogen bond or dispersion contact?. Physical Chemistry Chemical Physics, 2017, 19, 18194-18200.	2.8	32
39	Explicit treatment of active-site waters enhances quantum mechanical/implicit solvent scoring: Inhibition of CDK2 by new pyrazolo[1,5-a]pyrimidines. European Journal of Medicinal Chemistry, 2017, 126, 1118-1128.	5.5	32
40	Pnictogen bonding in pyrazine•PnX5 (Pn = P, As, Sb and X = F, Cl, Br) complexes. Journal of Molecular Modeling, 2017, 23, 328.	1.8	18
41	A novel stibacarbaborane cluster with adjacent antimony atoms exhibiting unique pnictogen bond formation that dominates its crystal packing. Dalton Transactions, 2017, 46, 13714-13719.	3.3	14
42	Mimicking of cyproconazole behavior in the presence of Cu and Zn. Rapid Communications in Mass Spectrometry, 2017, 31, 2043-2050.	1.5	8
43	Superior Performance of the SQM/COSMO Scoring Functions in Native Pose Recognition of Diverse Protein–Ligand Complexes in Cognate Docking. ACS Omega, 2017, 2, 4022-4029.	3.5	22
44	Nuclear Magnetic Shielding of Monoboranes: Calculation and Assessment of ¹¹ B NMR Chemical Shifts in Planar BX ₃ and in Tetrahedral [BX ₄] ^{â^'} Systems. Journal of Physical Chemistry A, 2017, 121, 9631-9637.	2.5	10
45	The Interplay between Various σ- and π-Hole Interactions of Trigonal Boron and Trigonal Pyramidal Arsenic Triiodides. Crystals, 2017, 7, 225.	2.2	6
46	IDD388 Polyhalogenated Derivatives as Probes for an Improved Structure-Based Selectivity of AKR1B10 Inhibitors. ACS Chemical Biology, 2016, 11, 2693-2705.	3.4	19
47	Competition between Halogen, Hydrogen and Dihydrogen Bonding in Brominated Carboranes. ChemPhysChem, 2016, 17, 3373-3376.	2.1	40
48	5-Substituted Pyrimidine and 7-Substituted 7-Deazapurine dNTPs as Substrates for DNA Polymerases in Competitive Primer Extension in the Presence of Natural dNTPs. ACS Chemical Biology, 2016, 11, 3165-3171.	3.4	63
49	Chalcogens act as inner and outer heteroatoms in borane cages with possible consequences for I_f -hole interactions. CrystEngComm, 2016, 18, 8982-8987.	2.6	8
50	Ab initio and DFT studies of the interaction between carbonyl and thiocarbonyl groups: the role of S···O chalcogen bonds. Theoretical Chemistry Accounts, 2016, 135, 1.	1.4	13
51	The π Complex of the Hydronium Ion Frozen on the Pathway of Electrophilic Aromatic Substitution. European Journal of Organic Chemistry, 2016, 2016, 4473-4475.	2.4	2
52	The SQM/COSMO filter: reliable native pose identification based on the quantum-mechanical description of protein–ligand interactions and implicit COSMO solvation. Chemical Communications, 2016, 52, 3312-3315.	4.1	55
53	The non-planarity of the benzene molecule in the X-ray structure of the chelated bismuth(iii) heteroboroxine complex is not supported by quantum mechanical calculations. Dalton Transactions, 2016, 45, 462-465.	3.3	10
54	Substrate Specificity, Inhibitor Selectivity and Structure-Function Relationships of Aldo-Keto Reductase 1B15: A Novel Human Retinaldehyde Reductase. PLoS ONE, 2015, 10, e0134506.	2.5	17

#	Article	IF	CITATIONS
55	Noncovalent Interactions of Heteroboranes. Challenges and Advances in Computational Chemistry and Physics, 2015, , 219-239.	0.6	4
56	Chalcogen and Pnicogen Bonds in Complexes of Neutral Icosahedral and Bicapped Square-Antiprismatic Heteroboranes. Journal of Physical Chemistry A, 2015, 119, 1388-1395.	2.5	39
57	The properties of substituted 3D-aromatic neutral carboranes: the potential for σ-hole bonding. Physical Chemistry Chemical Physics, 2015, 17, 20814-20821.	2.8	26
58	The Effect of Halogen-to-Hydrogen Bond Substitution on Human Aldose Reductase Inhibition. ACS Chemical Biology, 2015, 10, 1637-1642.	3.4	45
59	Malonate-based inhibitors of mammalian serine racemase: Kinetic characterization and structure-based computational study. European Journal of Medicinal Chemistry, 2015, 89, 189-197.	5.5	49
60	Structural and Functional Studies of Phosphoenolpyruvate Carboxykinase from Mycobacterium tuberculosis. PLoS ONE, 2015, 10, e0120682.	2.5	7
61	Carborane-Based Carbonic Anhydrase Inhibitors: Insight into CAII/CAIX Specificity from a High-Resolution Crystal Structure, Modeling, and Quantum Chemical Calculations. BioMed Research International, 2014, 2014, 1-9.	1.9	18
62	The Dominant Role of Chalcogen Bonding in the Crystal Packing of 2D/3D Aromatics. Angewandte Chemie, 2014, 126, 10303-10306.	2.0	26
63	Structural Basis for Inhibition of Mycobacterial and Human Adenosine Kinase by 7-Substituted 7-(Het)aryl-7-deazaadenine Ribonucleosides. Journal of Medicinal Chemistry, 2014, 57, 8268-8279.	6.4	26
64	The Dominant Role of Chalcogen Bonding in the Crystal Packing of 2D/3D Aromatics. Angewandte Chemie - International Edition, 2014, 53, 10139-10142.	13.8	124
65	Theoretical insight into the stabilization of triazole fungicides via their interactions with dications. International Journal of Mass Spectrometry, 2014, 359, 38-43.	1.5	12
66	7â€Arylâ€7â€deazaadenine 2′â€Deoxyribonucleoside Triphosphates (dNTPs): Better Substrates for DNA Polymerases than dATP in Competitive Incorporations. Angewandte Chemie - International Edition, 2014, 53, 7552-7555.	13.8	61
67	The Dominant Role of Chalcogen Bonding in the Crystal Packing of 2D/3D Aromatics. Angewandte Chemie - International Edition, 2014, 53, 10139-10142.	13.8	1
68	Quantum Mechanical Scoring: Structural and Energetic Insights into Cyclin-Dependent Kinase 2 Inhibition by Pyrazolo[1,5-a]pyrimidines. Current Computer-Aided Drug Design, 2013, 9, 118-129.	1.2	5
69	Quantum Mechanics-Based Scoring Rationalizes the Irreversible Inactivation of Parasitic <i>Schistosoma mansoni</i> Cysteine Peptidase by Vinyl Sulfone Inhibitors. Journal of Physical Chemistry B, 2013, 117, 14973-14982.	2.6	43
70	QM/MM Calculations Reveal the Different Nature of the Interaction of Two Carborane-Based Sulfamide Inhibitors of Human Carbonic Anhydrase II. Journal of Physical Chemistry B, 2013, 117, 16096-16104.	2.6	47
71	Modulation of Aldose Reductase Inhibition by Halogen Bond Tuning. ACS Chemical Biology, 2013, 8, 2484-2492.	3.4	85
72	The Semiempirical Quantum Mechanical Scoring Function for In Silico Drug Design. ChemPlusChem, 2013, 78, 921-931.	2.8	80

#	Article	IF	CITATIONS
73	Synthesis of nucleosides and dNTPs bearing oligopyridine ligands linked through an octadiyne tether, their incorporation into DNA and complexation with transition metal cations. Organic and Biomolecular Chemistry, 2013, 11, 78-89.	2.8	9
74	Assessing the Accuracy and Performance of Implicit Solvent Models for Drug Molecules: Conformational Ensemble Approaches. Journal of Physical Chemistry B, 2013, 117, 5950-5962.	2.6	60
75	Halogen bond tunability II: the varying roles of electrostatic and dispersion contributions to attraction in halogen bonds. Journal of Molecular Modeling, 2013, 19, 4651-4659.	1.8	190
76	Quantum Mechanical Scoring: Structural and Energetic Insights into Cyclin-Dependent Kinase 2 Inhibition by Pyrazolo[1,5-a]pyrimidines. Current Computer-Aided Drug Design, 2013, 9, 118-129.	1.2	52
77	Structural Basis for Inhibition of Cathepsin B Drug Target from the Human Blood Fluke, Schistosoma mansoni. Journal of Biological Chemistry, 2011, 286, 35770-35781.	3.4	60
78	On the reliability of the corrected semiempirical quantum chemical method (PM6-DH2) for assigning the protonation states in HIV-1 protease/inhibitor complexes. Collection of Czechoslovak Chemical Communications, 2011, 76, 457-479.	1.0	7
79	Semiempirical Quantum Mechanical Method PM6-DH2X Describes the Geometry and Energetics of CK2-Inhibitor Complexes Involving Halogen Bonds Well, While the Empirical Potential Fails. Journal of Physical Chemistry B, 2011, 115, 8581-8589.	2.6	80
80	Ligand Conformational and Solvation/Desolvation Free Energy in Proteinâ^'Ligand Complex Formation. Journal of Physical Chemistry B, 2011, 115, 4718-4724.	2.6	24
81	Transferable scoring function based on semiempirical quantum mechanical PM6-DH2 method: CDK2 with 15 structurally diverse inhibitors. Journal of Computer-Aided Molecular Design, 2011, 25, 223-235.	2.9	48
82	Halogen bond tunability I: the effects of aromatic fluorine substitution on the strengths of halogen-bonding interactions involving chlorine, bromine, and iodine. Journal of Molecular Modeling, 2011, 17, 3309-3318.	1.8	374
83	Inhibition of human purine nucleoside phosphorylase by tenofovir phosphate congeners. Collection of Czechoslovak Chemical Communications, 2010, 75, 1249-1257.	1.0	3
84	Interactions of Boranes and Carboranes with Aromatic Systems: CCSD(T) Complete Basis Set Calculations and DFT-SAPT Analysis of Energy Components. Journal of Physical Chemistry A, 2010, 114, 11304-11311.	2.5	31
85	A Reliable Docking/Scoring Scheme Based on the Semiempirical Quantum Mechanical PM6-DH2 Method Accurately Covering Dispersion and H-Bonding: HIV-1 Protease with 22 Ligands. Journal of Physical Chemistry B, 2010, 114, 12666-12678.	2.6	116
86	Synthesis of Analogues of Acyclic Nucleoside Diphosphates Containing a (Phosphonomethyl)phosphanyl Moiety and Studies of Their Phosphorylation. European Journal of Organic Chemistry, 2009, 2009, 1082-1092.	2.4	7
87	Semiempirical Quantum Chemical PM6 Method Augmented by Dispersion and H-Bonding Correction Terms Reliably Describes Various Types of Noncovalent Complexes. Journal of Chemical Theory and Computation, 2009, 5, 1749-1760.	5.3	312
88	Stimuli-Responsive Nanoparticles Based on Interaction of Metallacarborane with Poly(ethylene oxide). Macromolecules, 2009, 42, 4829-4837.	4.8	40
89	Design of HIV Protease Inhibitors Based on Inorganic Polyhedral Metallacarboranes. Journal of Medicinal Chemistry, 2009, 52, 7132-7141.	6.4	132
90	Interpretation of Protein/Ligand Crystal Structure using QM/MM Calculations: Case of HIV-1 Protease/Metallacarborane Complex. Journal of Physical Chemistry B, 2008, 112, 15094-15102.	2.6	52

#	Article	IF	CITATIONS
91	Inorganic Polyhedral Metallacarborane Inhibitors of HIV Protease: A New Approach to Overcoming Antiviral Resistance. Journal of Medicinal Chemistry, 2008, 51, 4839-4843.	6.4	90
92	Interaction of heteroboranes with biomolecules : Part 2. The effect of various metal vertices and exo-substitutions. Physical Chemistry Chemical Physics, 2007, 9, 2085-2093.	2.8	39
93	Interaction of Carboranes with Biomolecules: Formation of Dihydrogen Bonds. ChemPhysChem, 2006, 7, 1100-1105.	2.1	134
94	Hydration Gibbs Energies of Nucleic Acid Bases Determined by Gibbs Energy Perturbation, Continuous and Hybrid Approaches. Collection of Czechoslovak Chemical Communications, 2005, 70, 1756-1768.	1.0	3